



U.S. DEPARTMENT OF
ENERGY

PNNL-20808

Prepared for the U.S. Department of Energy
under Contract DE-AC05-76RL01830

Risk-Informed Monitoring, Verification and Accounting (RI-MVA)

An NRAP White Paper Documenting Methods and a Demonstration Model for
Risk-Informed MVA System Design and Operations in Geologic Carbon
Sequestration

SD Unwin
A Sadovsky

C Sullivan
RM Anderson

September 2011



Pacific Northwest
NATIONAL LABORATORY

*Proudly Operated by **Battelle** Since 1965*

DISCLAIMER

This report was prepared as an account of work sponsored by an agency of the United States Government. Neither the United States Government nor any agency thereof, nor Battelle Memorial Institute, nor any of their employees, makes **any warranty, express or implied, or assumes any legal liability or responsibility for the accuracy, completeness, or usefulness of any information, apparatus, product, or process disclosed, or represents that its use would not infringe privately owned rights.** Reference herein to any specific commercial product, process, or service by trade name, trademark, manufacturer, or otherwise does not necessarily constitute or imply its endorsement, recommendation, or favoring by the United States Government or any agency thereof, or Battelle Memorial Institute. The views and opinions of authors expressed herein do not necessarily state or reflect those of the United States Government or any agency thereof.

PACIFIC NORTHWEST NATIONAL LABORATORY

operated by

BATTELLE

for the

UNITED STATES DEPARTMENT OF ENERGY

under Contract DE-AC05-76RL01830

Printed in the United States of America

Available to DOE and DOE contractors from the
Office of Scientific and Technical Information,
P.O. Box 62, Oak Ridge, TN 37831-0062;
ph: (865) 576-8401
fax: (865) 576-5728
email: reports@adonis.osti.gov

Available to the public from the National Technical Information Service
5301 Shawnee Rd., Alexandria, VA 22312
ph: (800) 553-NTIS (6847)
email: orders@ntis.gov <<http://www.ntis.gov/about/form.aspx>>
Online ordering: <http://www.ntis.gov>

Risk-Informed Monitoring, Verification and Accounting (RI-MVA)

Table of Contents

Abstract	4
1. Introduction	4
2. Optimization Techniques and Sensor Network Design	5
3. General Risk Formulation	6
4. Monitoring System Characterization	11
5. Risk-Informed Optimization Principles	12
6. Optimization and Simulated Annealing	13
7. Demonstration Model	16
8. Conclusions	22
9. Future Steps	23
10. References	24
Appendix 1: Precedents in Sensor Network Optimization Methods	28
Appendix 2: Supplementary Technical Details	32

Abstract

This white paper accompanies a demonstration model that implements methods for the risk-informed design of monitoring, verification and accounting (RI-MVA) systems in geologic carbon sequestration projects. The intent is that this model will ultimately be integrated with, or interfaced with, the National Risk Assessment Partnership (NRAP) integrated assessment model (IAM). The RI-MVA methods described here apply optimization techniques in the analytical environment of NRAP risk profiles to allow systematic identification and comparison of the risk and cost attributes of MVA design options.

1. Introduction

A prime objective of the National Risk Assessment Partnership (NRAP) is the development of methodological and modeling resources to help ensure that carbon sequestration technologies are reliable, effective, and safe [NETL, 2011]. To achieve this objective, the new generation of risk methods that emerge from NRAP will meet a broad set of decision-making demands, including integrated, strategic, risk-based monitoring and mitigation protocols.

Well-designed monitoring, verification and accounting (MVA) systems will ultimately serve to narrow the uncertainties associated with sequestration risk. Conversely, risk insights have the potential to inform the design and operation of MVA systems. Risk-informed MVA (RI-MVA) design is the focus of this white paper. Specifically, a methodological framework for RI-MVA compatible with the NRAP Integrated Assessment Model (IAM) is described. To demonstrate this framework, a rapid prototype analytical tool has been developed.

MVA is a major cost component of geologic sequestration and systematic identification of MVA options along with their risk implications will provide a key basis for assessing MVA cost-efficacy. The methodology and demonstration tool described in this white paper incorporate optimization methods that facilitate understanding of the risk profiles of optional MVA strategies and designs, as well as providing the means of establishing the tradeoffs between risks and costs.

2. Optimization Techniques and Sensor Network Design

There is substantial precedent for the application of mathematical optimization techniques to the design of sensor networks and monitoring systems. One historic focus has been on analytical frameworks for the design of sensor networks in drinking water distribution systems, with optimization objectives that include contamination detection times and sizes of affected populations [Ostfeld et al, 2006; Storck et al., 1997; Krause et al. 2008]. National security is another domain that has made significant investment in developing methods to optimize sensor network designs [Zou and Chakrabarty, 2004]. There does exist precedent for use of optimization principles in the design of sensor networks serving geologic storage systems [Houston, 2000]; some specifically oriented to carbon sequestration [Saripalli et al., 2006]. Appendix 1 provides a fuller account of precedents in sensor network design optimization.

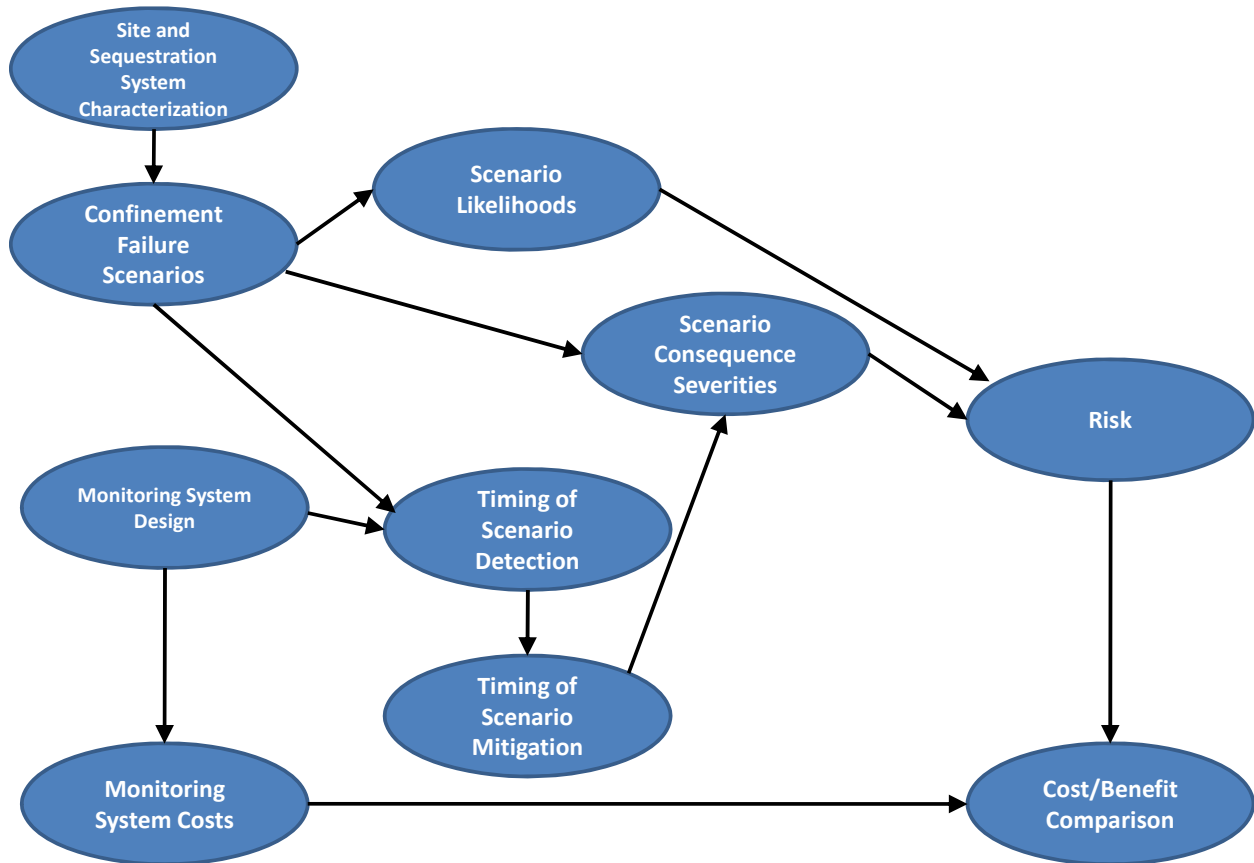
Drawing on these precedents, the intent here is to develop optimization algorithms that are explicitly risk-based and that reflect the risk metrics, methods, models, priorities, and insights being identified under the NRAP program. There are numerous categories of risk and prospective risk metrics associated with geologic carbon sequestration. NRAP has selected a set of impact categories as the near-term focus of risk characterization [NETL, 2011]. These are:

- (1) Return of CO₂ to the atmosphere
- (2) Degradation of groundwater quality
- (3) Impacts on the geosphere such as nuisance or destructive induced seismicity.

For the purposes of RI-MVA methodology and tool development, our principal focus will be on the risk associated with scenarios involving confinement failure of the primary reservoir and associated consequence metrics.

The general form of the RI-MVA framework to be described is captured in Figure 2-1. The efficacies and reliabilities with which various confinement failure scenarios are detected or pre-empted are determined for a large set of MVA design alternatives. In the setting of a risk model, the potential degrees of mitigation associated with confinement failure scenarios are then assessed for each MVA alternative, and this provides a basis for comparison of MVA system costs to risk-reduction benefit.

Figure 2-1.
The RI-MVA Framework

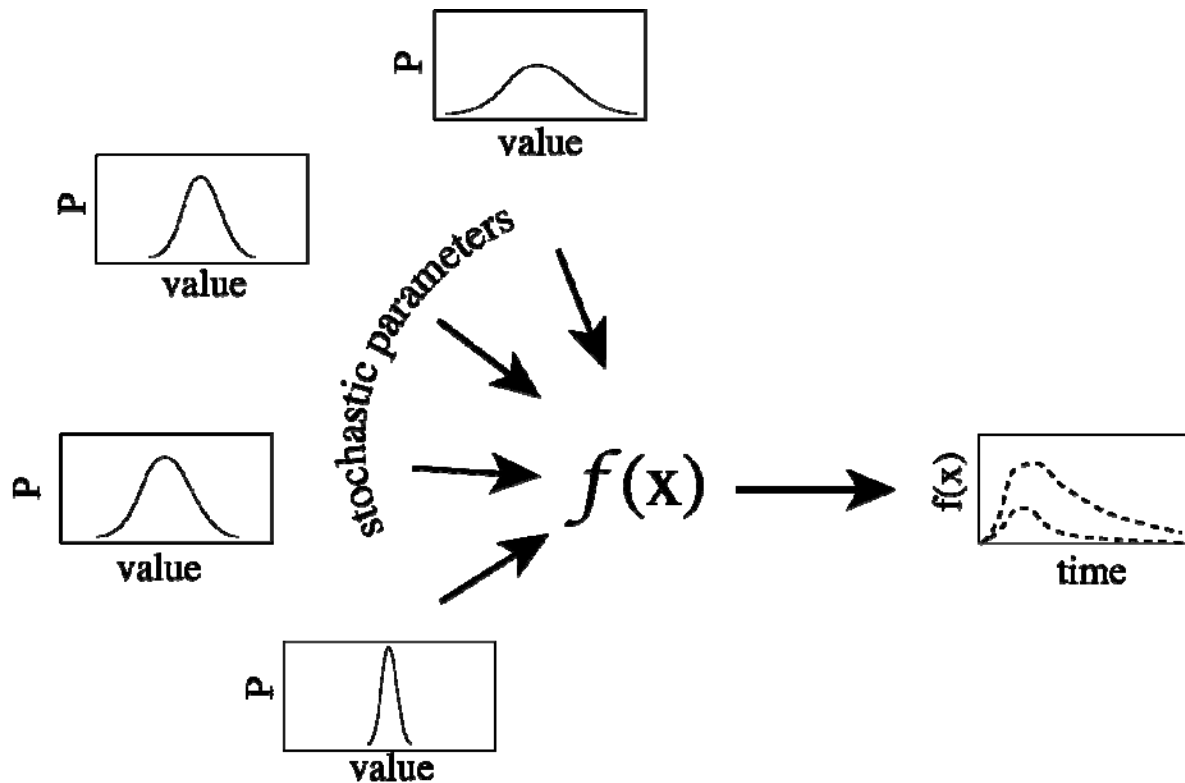


3. General Risk Formulation

In FY11 the NRAP program produced a set of preliminary risk profiles. By the end of CY11, the intent is to develop an integrated assessment model (IAM) that incorporates uncertainty quantification and provides the platform for a full set of first generation risk profiles. Our objective is to develop an RI-MVA framework that will be compatible with the NRAP IAM. Since the specific form of the IAM is yet to be fully established, the methods defined in this white paper are based on projections of its likely form. However, the RI-MVA methodology will be sufficiently robust to accommodate a range of IAM structures.

Underlying the first generation risk profiles will be a set of deterministic hydrologic, geologic, mineralogic and chemical models that address the phenomena associated with primary reservoir behavior, wellbore leakage, natural pathway leakage, and aquifer response. Uncertainties associated with the magnitudes of the input parameters to the models will be represented by probability distributions. The distributions will then be propagated through the integrated suite of models to determine the probability distributions over the output consequence metrics, such as the spatial and temporal distributions of pH levels and total dissolved solids (TDS) in shallow aquifers. Figure 3-1 represents this conceptual process.

Figure 3-1.
 Calculational Framework for NRAP Risk/Uncertainty Analysis
 [from NETL, 2011]



Numerical methods – Monte Carlo analysis – will be used to propagate the probability distributions through the models, likely using the GoldSim platform [GoldSim Technology Group, 2006]. Given the substantial run-times associated with some of the source science models, it is likely that faster-running surrogate models will be used

for the integrated analyses. These surrogate models may be based either on statistical response surfaces that emulate with adequate fidelity the input/output behavior of the underlying models [Iman and Conover, 1980], or on reduced form physical models that simplify the formulations of the underlying science.

The scenarios addressed in the model will involve reservoir confinement failure mechanisms such as

- caprock permeation
- leaky wellbores
- existing transmissive faults or fracture zones
- induced faults or fractures,

along with the potential migration paths and mechanisms determined by the connectivity of the confinement failure locations to the volumetric endpoints of interest [Oldenburg et al., 2009]. In the first generation risk profiles, the endpoints will be:

- underground sources of drinking water
- surface water
- atmosphere.

Based on an analysis such as that represented in Figure 3-1, the typical output of the IAM will take the general form of a joint probability distribution $P(\underline{C})$ over some vector of consequence metrics, \underline{C} , which would include, for example, time-dependent pH and TDS levels defined at various volumetric endpoints (compartments, in the vernacular of the Certification Framework [Oldenburg et al., 2009]).

The probability density $P(\underline{C})$ can then form the basis for several representations of risk. The most conventional representation has the form

$$\text{Risk} = \text{Probability} \times \text{Consequence}, \quad (1)$$

where a vector of risk indices is expressed as

$$R_i = \int P_i(C_i) C_i dC_i \quad (2)$$

R_i is the risk with respect to the i 'th consequence metric, C_i , and P_i is the marginal probability distribution over C_i . In essence, this risk is equal to the expectation value of

the consequence metric under the uncertainties associated with the model input parameters. An alternative and common characterization of risk is the complementary cumulative distribution function (CCDF) associated with the marginal probability density; that is,

$$CCDF_i(C_i) = \int_{C_i}^{\infty} P_i(C_i') dC_i' \quad (3)$$

which represents exceedence probabilities for various levels of consequence severity. These characterizations of risk can be viewed as the accumulation of risk contributions from a set of confinement failure scenarios and subsequent leak paths.

To this point we assume that the confinement failure scenarios are unmitigated. That is, in these representations of risk, no credit has been taken for mitigative actions. Now consider the presence of an MVA system with the design objective of identifying anomalies associated with potential confinement failures. In principle, the detection of such failures would prompt response actions intended to mitigate the impact. (Halting injection would be a key mitigative action. Additional means of mitigation will be a future focus for NRAP.) Therefore, the risk model could be modified to take credit for prospective mitigation actions once a confinement failure is detected. In this case (starting with Equation 2) we have

$$R'_i = \int P'_i(C_i) C_i dC_i \quad (4)$$

where the prime attached to the risks and probability densities indicates that mitigative actions have been accounted for, and the associated reduction in consequence severities for each scenario have been incorporated into the integrated model.

The degree to which a confinement failure can be mitigated will depend on the efficacy and reliability of the MVA system in place to detect the failure. For example, the timeliness of anomaly detection would be one factor expected to drive both the degree to which mitigation is practical, and the potential efficacy of mitigative response. Therefore, Equation 4 can be re-expressed as

$$R_{ik} = \int P_{ik}(C_i) C_i dC_i \quad (5)$$

where the index k enumerates MVA system design and operational options; that is, Equation 5 expresses risk as a function of the MVA design option. If Equation 5 were

implementable, then it would be the basis for risk-informed MVA design. Implementation would require:

1. modeling the performance of optional MVA systems/configurations relative to the range of scenarios and conditions identified in the underlying physical models, and
2. modeling the operator's decision-making and mitigative response actions subject to inferences made from MVA.

While future NRAP activity will focus on mitigation, we make some tentative assumptions here to allow near-term progress on the RI-MVA framework. We assume first that a key determinant of the potential to mitigate a confinement failure scenario is the timing of anomaly detection. That is, the greater the time to detection, the greater the impact of a scenario is likely to be. While we would expect a monotonic relationship between time to detection and consequence severity, the specific nature of that relationship is yet to be established. As an interim, surrogate measure of consequence severity, we can use the time to detection itself. That is we define the following as a surrogate risk measure:

$$R_k = \int P_k(t) t dt \tag{6}$$

where t is the time interval between confinement failure and anomaly detection, and k is an index that enumerates the MVA design options.

As noted earlier, the propagation of uncertainty in NRAP methodology is based on Monte Carlo methods. That is, Equation 6 would be implemented by numerical methods and the output of the risk analysis would be a sample of values of a given output consequence metric from which its probability distribution can be constructed. Each sample member represents a single, quantitative realization of all input parameters to the physical models. The means of integrating such a risk model with the RI-MVA framework resides in establishing the time to confinement failure detection for the physical conditions realized in each sample member (that is, for those sample members that involve confinement failure) and for each MVA option. This forms the basis for implementing Equation 6.

4. Monitoring System Characterization

A given MVA system option is assumed to be defined by a network of sensors of varying technologies/types, deployment timings, and locations (fixed and dynamic) [NETL, 2009]. In general sensor types might include:

- Atmospheric monitoring
 - Direct CO₂ detectors
 - LIDAR
 - Tracers
 - Eddy covariance

- Near Surface monitoring
 - Areal optical methods (including satellite imagery)
 - Tracers
 - Groundwater monitoring (head, chemistry)
 - Soil gas monitoring
 - Electrical, including resistivity, Sp, induced polarization

- Subsurface monitoring
 - Surface and cross-well multi-component seismic time-lapse
 - Magneto-telluric sounding
 - Deep electromagnetic induction tomography
 - Time-lapse gravity
 - Vertical seismic time-lapse
 - Ground deformation (tiltmeters, InSAR, microgravity)
 - Well logging of electrical, acoustical or chemical properties, fluid saturations, cement bond
 - Microseismic activity (induced seismic)
 - Mechanical well integrity tests
 - Annulus Pressure
 - Fluid chemistry

For the purposes of the RI-MVA demonstration model, two sensor types are considered: direct CO₂ detectors and pressure sensors. The model is principally concerned with two sensor attributes: cost (ultimately, both the initial capital cost and periodic operating or maintenance costs) and the threshold for detection. In brief, the threshold is the minimum stimulus level to which a sensor is exposed such that the

operator concludes that an anomalous event has occurred. It is not, however, the minimum stimulus required to infer confinement failure. Inference of confinement failure is assumed to require an appropriate combination of anomalous events (confirmatory data), as specified by the RI-MVA inference model.

For a given distribution of sensors, the RI-MVA model estimates the time to anomaly detection for each Monte Carlo output sample member generated by the risk model; that is, for each realization of physical input parameters. An anomalous event is assumed to be the detection of a signal by a sensor that would (1) imply occurrence of a confinement failure scenario, or (2) prompt or focus additional monitoring activity to confirm or disconfirm that confinement failure has occurred. In general, we assume that there would need to be mutually-enforcing evidence or confirmatory output from multiple sensors to produce an inference that is sufficiently robust to support response actions. Since sensors would be expected to employ disparate technologies and rely upon differing physical stimuli, the basis for defining the thresholds for robust inferences will vary.

Sensor thresholds are not treated as static in RI-MVA. Rather, we allow a given sensor's thresholds to vary based on measurements obtained from other sensors. This is because multiple sensors may reinforce each other and provide greater evidence of anomalous activity than a single sensor. As defined previously, a sensor's threshold level is a measure of the evidence required to conclude that anomalous activity is occurring. The amount of evidence required from a given sensor is reduced if other sensors are providing confirmatory evidence. This dependency between sensors is captured in an inference model, which is a module within the larger RI-MVA model. More details of the inference model are contained in Appendix 2.

5. Risk-Informed Optimization Principles

There can be numerous alternative and complementary risk-informed decision criteria for MVA system design. In the demonstration analysis, the expectation value of the time to anomaly detection is the surrogate risk metric. This, in combination with consideration of the costs of each MVA option, would provide the basis for cost-benefit comparison. In a fuller analysis, design selection would address multi-attribute risks (as defined by risk metrics selected under NRAP) as well as system costs associated with installation, operation and maintenance. The current basis for addressing the cost component of the analysis is described in Section 7.

A key technical challenge for RI-MVA is the ability to systematically identify and analyze MVA design options. In principle, an optimization analysis would need to consider a space of options that spans sensor types, counts, physical configurations, and installation times. The characterization and exploration of this abstract, multi-dimensional space is not straightforward and presents the key challenge for the RI-MVA methodology – computational cost being a key factor. To explore that space and select MVA options, the analytical technique of *Simulated Annealing* has been adopted, as described in the following section.

6. Optimization and Simulated Annealing

Simulated annealing is a randomized optimization algorithm that iteratively searches through numerous candidate solutions until it converges to the “best” one – in this case, the option in which risk (the expected time to confinement failure detection) is minimized for a given system cost constraint. Built-into the algorithm are means of avoiding early convergence to local risk minima (that is, local in the option space), and this increases the likelihood that the resulting risk is a global minimum.

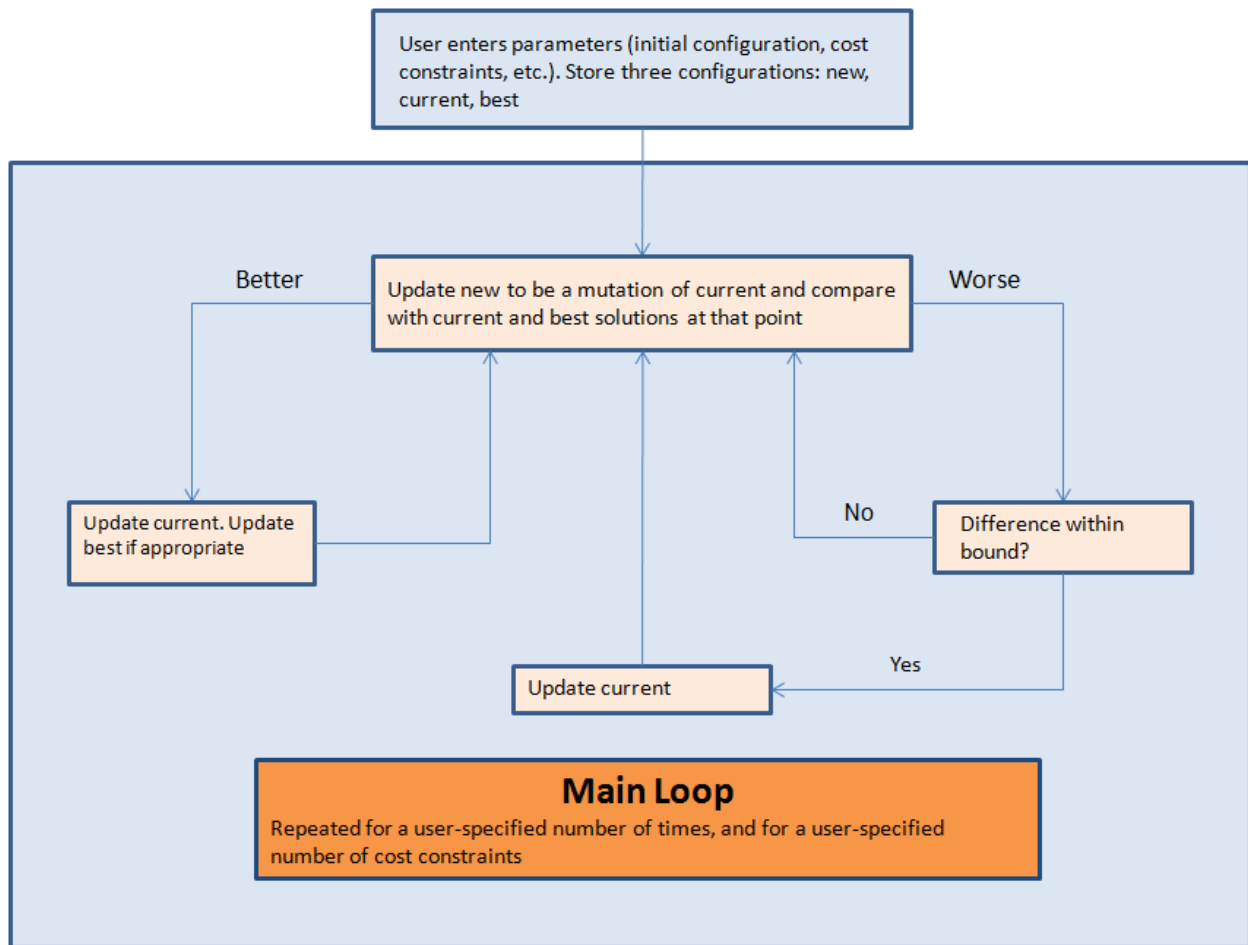
Central to the algorithm is a *mutation function*. This function sequentially generates a new candidate solution from the previous solution using a randomized approach. The particular form taken by the randomization is problem dependent: in our case, we randomly select sensor types and randomly alter their locations. The resulting new solution may or may not be better (lower risk) than the prior one from which it was mutated. So:

(1) If it is better, it is accepted as the starting point for subsequent mutations. It is also compared to the best solution found thus far. If it is better, then it is retained as the new best solution.

(2) If it is worse than the solution from which it is mutated, it is accepted as the next starting point provided that the difference between the risk associated with the current and previous solutions is less than a certain threshold level, which is defined as part of the algorithm. The purpose of accepting a worse solution is to allow the algorithm to periodically escape a local risk minimum. Note that the algorithm still retains memory of the best solution – this is only modified if the mutation is strictly better.

This process is represented in Figure 6-1.

**Figure 6-1.
Simulated Annealing Algorithm**



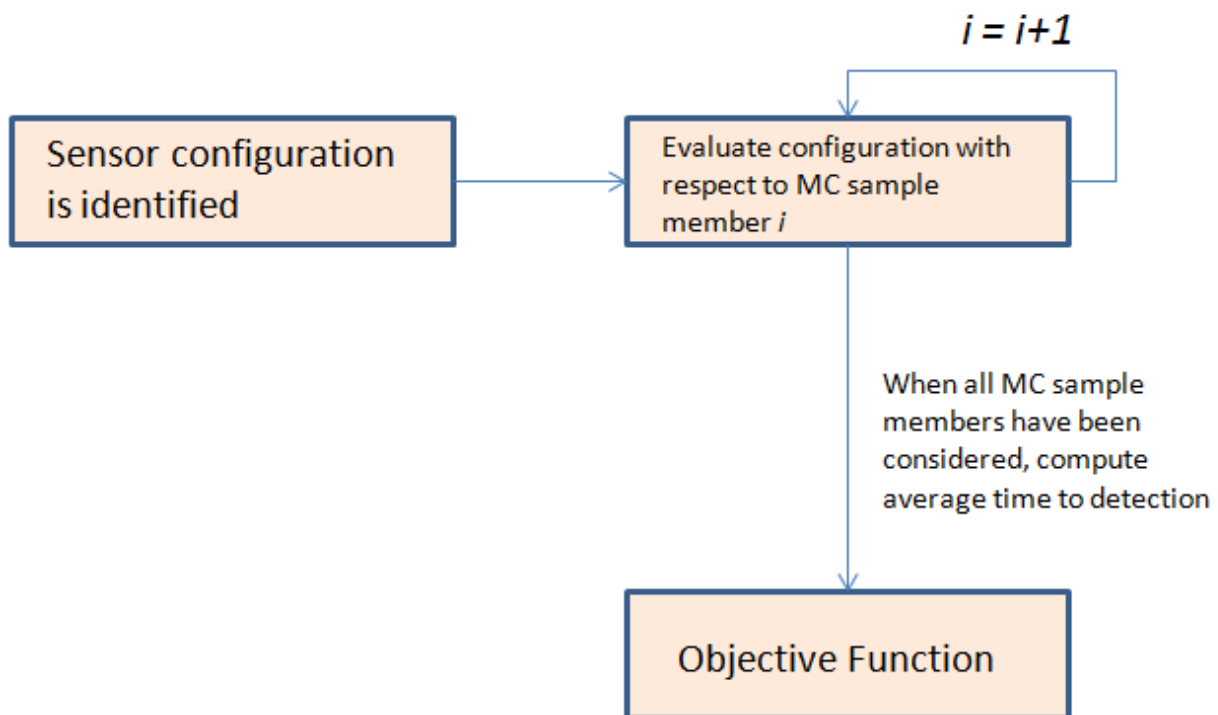
One of the major advantages of simulated annealing is that it does not require any particular functional form for the objective function (detection time). The only requirement is the ability to evaluate the objective function for various candidate solutions generated by the algorithm. As outlined in Appendix 2, the current problem involves an objective function that has no closed form representation, and this precludes the use of more conventional optimization techniques such as linear programming.

It should be noted that simulated annealing, like all randomized algorithms, cannot ensure convergence on identical solutions for multiple implementations. However, techniques do exist to increase the likelihood that the resulting configurations do in fact reflect the global risk minimum, or a good approximation to it. These techniques include adjustments to the number of allowed iterations and the modification of

internal algorithm parameters. These techniques are employed in the RI-MVA model. Overviews of simulated annealing algorithms can be found in Bertsimas and Tsitsiklis [1993] and Kirkpatrick et al [1983].

Note that the RI-MVA algorithm is designed to handle a large number of confinement failure scenarios. Each member of the Monte Carlo sample (from the underlying risk model) represents a scenario, or “state of the world”, selected from numerous alternative reservoir plume characteristics, confinement failure points/mechanisms, and release migration pathways. The sample data will be spatially and temporally indexed, which will allow us to evaluate the time to confinement failure detection for a particular configuration of sensors. The objective function used in the simulated annealing algorithm is the expectation value of the detection time (or, more generally, of the consequence metric) over the Monte Carlo sample. More detail of the process is in Appendix 2. Figure 6–2 illustrates how the Monte Carlo sample of times to confinement failure detection forms the basis for calculating the objective function – the mean time to detection.

Figure 6–2.
Monte Carlo Sample and the Objective Function

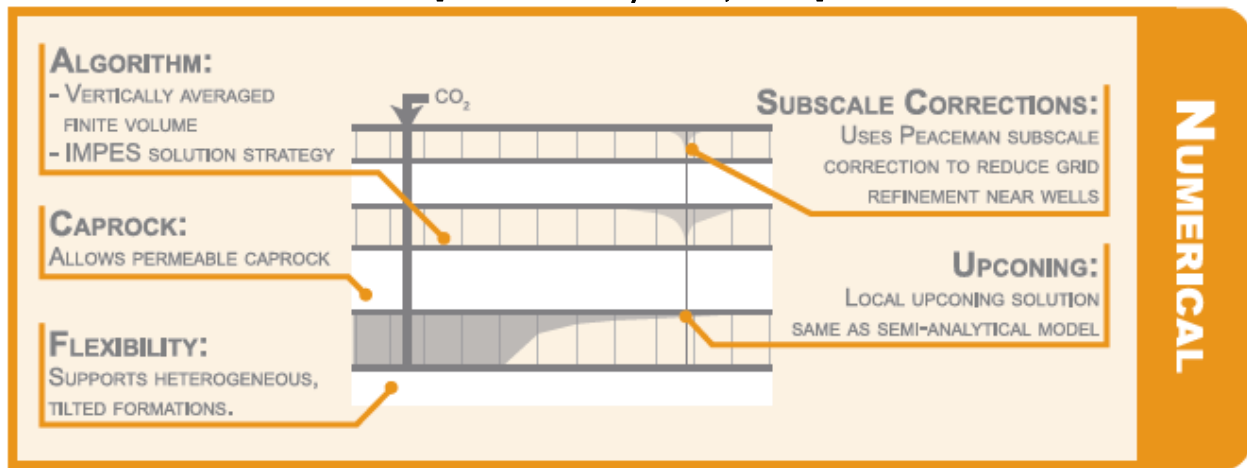


7. Demonstration Model

The NRAP integrated assessment model (IAM) will provide the ultimate basis for implementation of the RI-MVA methods described here. As an interim basis for implementing and calibrating the RI-MVA methods, Geological Storage Consultants, LLC (GSC) has shared a dataset representing a hypothetical confinement failure scenario. These data consist of spatial-temporal CO₂ concentrations, along with pressure field data, for cells defined in a hypothetical sequestration site. GSC generated the data using an efficient vertically averaged numerical model. Figure 7-1 represents the general structure of the model. Some salient aspects of the model are:

- The confinement failure mechanism is an abandoned permeable well.
- The site is modeled using two layers: one layer represents the reservoir, the other represents locations above the reservoir. Since we assume no sensors are placed in the reservoir, all sensors in the demo have a single depth coordinate. We expect future datasets to include multiple vertical strata, which RI-MVA is designed to accommodate.
- The original GSC data represent a single confinement failure location and a subsequent deterministic characterization of CO₂ migration. This can be viewed as equivalent to a single Monte Carlo sample member of data that would emerge from the NRAP risk model. To emulate additional Monte Carlo sample members, the GSC data were augmented with meta-data which was based on geographic translations of the confinement failure point in the original data. Five failure locations are thus represented, assumed to reflect a Monte Carlo sample of size 5.

Figure 7-1
 Illustration of the GSC Model
 [from Dobossy et al., 2010]



In addition to these features of the data, several simplifying assumptions have been made for the purposes of the model demonstration. These assumptions pertain to sensor characteristics, specifically the costing model and the basis for setting detection thresholds for the sensors:

- The emphasis of the demo project has been on establishing the calculational principles and algorithms for MVA design optimization rather than on the collection of supporting data for implementation. For current purposes, costs associated with various MVA designs have been denominated in arbitrary units. For example, CO₂ sensors and pressure sensors are associated with costs of 100 units and 150 units per sensor, respectively. It's also recognized that the structure of the costing model is currently simplistic and will require substantial refinement. For example, the current model simply adds the cost of individual sensors for a given configuration; whereas, more realistically, cost will be nonlinear and account for costs associated with the placement of the instrument wells required for a given configuration. Also, a more refined model will allow the explicit costing of system installation, operation, and maintenance.
- Sensor detection thresholds have been assigned nominal values for the demo model. These values were based on inspection of the GSC data set in conjunction with some preliminary judgments. Again, the emphasis of the demo is on establishing the calculational algorithms rather than on the collection of

supporting data. In collaboration with the MVA Working Group, more realistic sensor models will ultimately be established.

Operation

Figure 7–2 shows the RI–MVA data input screen. The algorithm requires the following user inputs:

- Initial sensor configuration: the user enters a series of sensors as the initial MVA design option. The sensors are defined in terms of their type (CO₂ and pressure sensors are current options) and location.
- Number of iterations: the simulated annealing algorithm involves iterative mutation of solutions to ultimately arrive at the “best” solution. The quality of the output depends on the number of iterations. However, there is a tradeoff: an excessive number of iterations is computationally expensive and may provide limited improvement in the solution.
- Cost constraints: the user also enters a total cost constraint on the MVA system. Cost is presently modeled as constraint on the solution, but the user has the option of incorporating cost into the objective function itself (see Appendix 2). The user has the option of adding alternative cost constraints, in which case the model sequentially uses these constraints to show the relationship between the risk minimum achieved and the total system cost.

Once the user has entered the required input, the algorithm is executed.

Figure 7-2.
Initial Input Screen

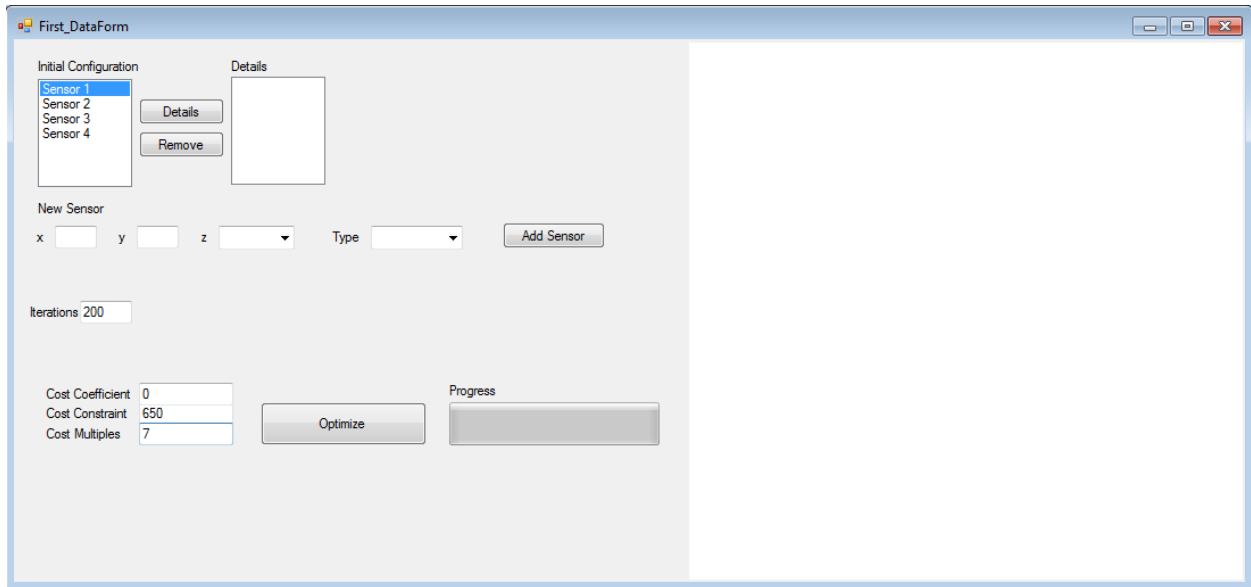
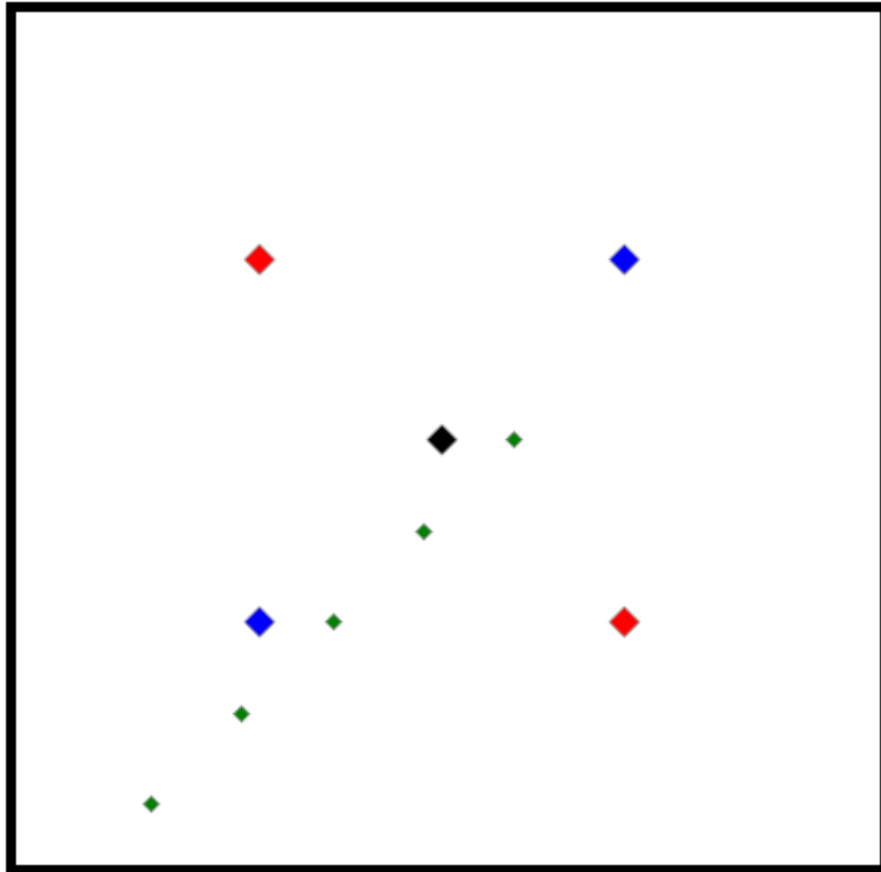


Figure 7-3 represents initiating data for the algorithm. The map shows a configuration of sensors – pressure sensors represented by blue diamonds and CO₂ sensors by red diamonds – the equiprobable confinement failure locations represented by green diamonds (representing a Monte Carlo sample of data from the risk model), and the injection point, represented by the black diamond. The initial user specified sensor configuration consists of four sensors that are equidistant from the injection point.

Figure 7-3.

Initial Configuration:

Black point is the injection location, green points are the equiprobable confinement failure locations, blue/red points are pressure/CO₂ sensors.



Results

When execution of the algorithm is complete, several sets of results are displayed. Figure 7-4 illustrates the optimal configuration determined by RI-MVA for a cost constraint of 650 units (30% greater than the cost of the initial configuration). The figure represents the configuration with the smallest probability-weighted confinement failure detection time for a cost no greater than 650 units. Comparison of Figures 7-3 and 7-4 reveals that sensors have been relocated closer to the confinement failure points, as would be expected. To interpret this optimized configuration, note that the top right confinement failure point results in the “most isotropic” leak pathways in the sense that CO₂ migration is distributed uniformly about the source point. In the other scenarios (i.e., the other four confinement failure locations) the direction of CO₂

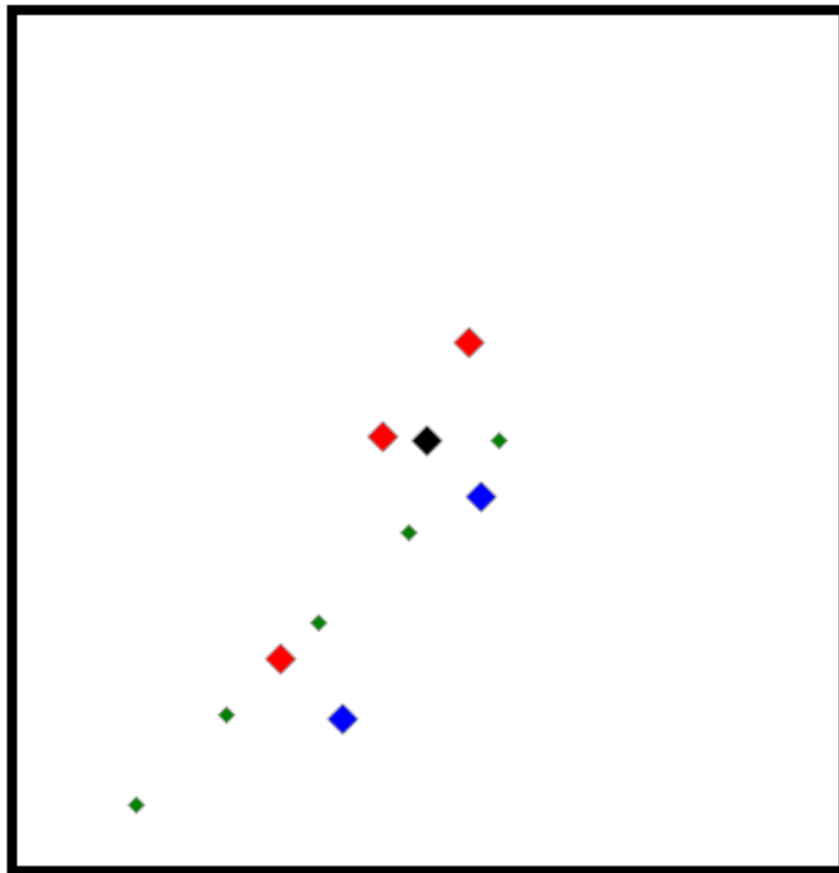
migration is predominantly to the right of the source. This anisotropy of CO₂ migration is reflected in the optimal sensor configuration.

An additional output is a comparison of the risk-minimized solutions to the initial user-provided configuration as a function of the allowable system costs. This is represented by graphs showing the risk and achievable risk reductions associated with increasing system cost (see Figure 7-5). Such data provide a transparent basis for cost-benefit analysis of MVA options. This basis will become more robust once the surrogate risk measure of expected time to detection is replaced by a more meaningful risk metrics.

Figure 7-4.

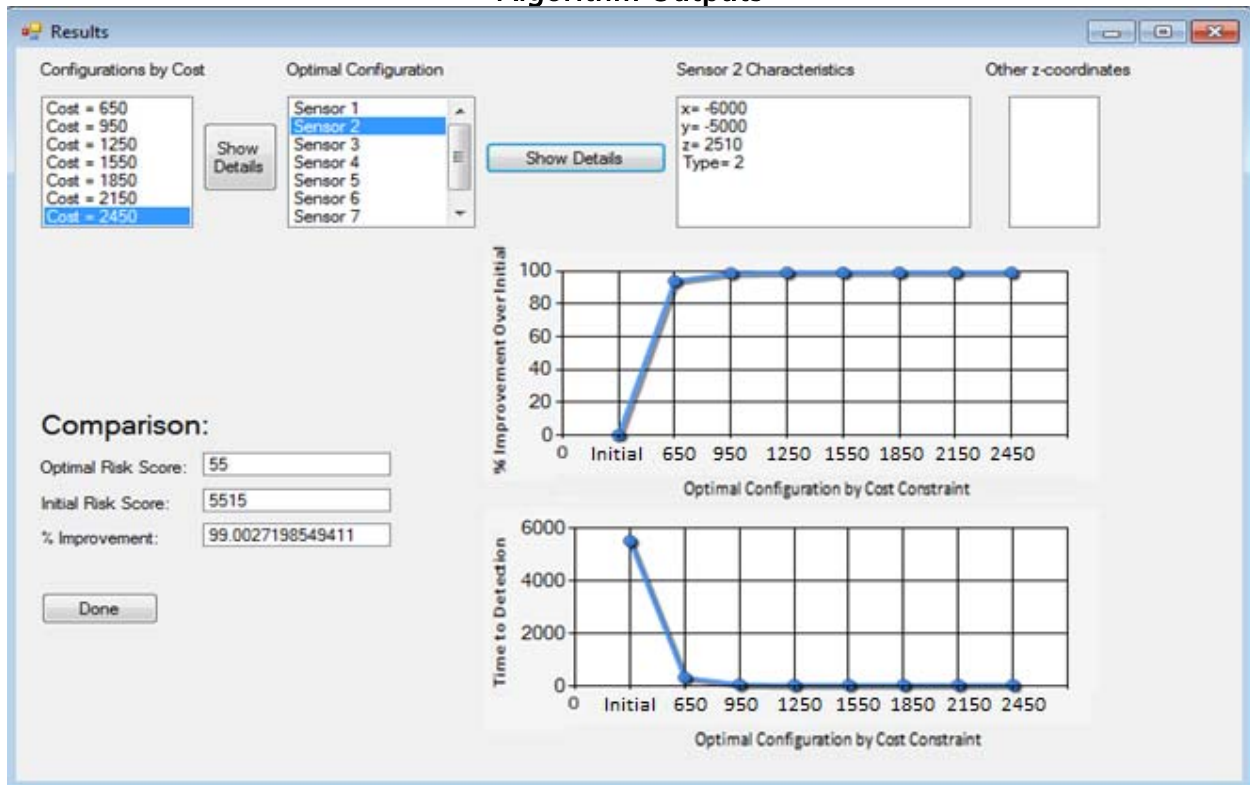
Risk-Minimized Configuration for a Cost Constraint 650 Units:

Black point is the injection location, green points are the equiprobable confinement failure locations, blue/red points are pressure/CO₂ sensors.



As expected, higher allowable costs result in lower-risk solutions; however, Figure 7–5 clearly shows the diminishing returns as allowable cost is increased. The top graph shows the percent improvement in the optimal configuration relative to the initial, user–provided configuration, as a function of cost constraint. The bottom graph shows the optimal configuration’s risk score (expected time to detection) as a function of the cost constraint. We see that for the best configuration at a cost constraint of 2,450 units, the minimum risk score is 55 days (the expected time between confinement failure and detection of the failure), a 99% improvement over the initial risk score. The optimal configuration for a cost constraint of only 650 units also yields a very significant improvement over the initial configuration. A cost–benefit analysis in this hypothetical case might suggest that expenditure beyond 650 units is unwarranted.

Figure 7–5.
Algorithm Outputs



8. Conclusions

The principles and features of an approach to risk–informed MVA (RI–MVA) system design and operations have been described, along with supporting optimization algorithms. Through leveraging and extending existing methodologies for sensor

network optimization, a rapid prototype model has been developed that is oriented towards integration with the NRAP IAM. A demonstration application of the model indicates that RI-MVA has the potential to provide a systematic, risk-informed basis for facilitating the cost-effective design of MVA systems. By ongoing collaboration with the NRAP working groups, the intent is to refine the RI-MVA model through:

1. Replacing the surrogate risk metrics and surrogate risk model with the IAM and its associated risk metrics as they emerge, and
2. Making refinements to RI-MVA model with respect to factors such as sensor definitions, MVA operational strategy, anomaly inference modeling, and system costing.

In the next section, some specific areas of improvement are identified.

9. Future Steps

Planned refinements to RI-MVA include –

1. Sensor definitions: The inventory of sensor types available to RI-MVA will be expanded and sensor capability will be more realistically modeled.
2. Data sampling: Strategies for sensor data sampling will be more realistically modeled, thus improving the basis for estimating the timing of anomaly detection.
3. Dynamic MVA design: The ability to model the phased deployment of sensors will be incorporated, accounting for evolving knowledge of plume characteristics.
4. System costing: Realistic bases for design option costing will be incorporated into RI-MVA, addressing installation, operational, and maintenance elements.
5. Inference and mitigation models: The operational inference and response models will be refined to more realistically reflect anomaly diagnostics, confirmatory analyses, and associated mitigative actions.

6. Sensor reliabilities: Included in the risk model will be scenarios in which sensors fail to meet their design intents.
7. IAM interface: RI-MVA analytical interfaces will be developed to reflect the emerging structure and metrics of the IAM.

10. References

- Aral, M., J. Guan, and M. Masila. 2008. "A multi-objective optimization algorithm for the solution of water sensor placement problem in water distribution systems." *Proceedings of the World Water and Environmental Resources Congress, ASCE/EWRI*, Honolulu, Hawaii, May 12–16, 2008.
- Barrett, S. 2007. "Optimizing sensor placement for intruder detection with genetic algorithms." *IEEE International Conference on Intelligence and Security Informatics*, pp. 185–188, May, 2007.
- Berry, J., E. Boman, L. Riesen, W. Hart, C. Phillips, J. Watson, and R. Murray. 2008. "TEVA-SPOT Toolkit and user's manual." U.S. Environmental Protection Agency, Washington D.C., EPA/600/R-08/041A.
- Bertsimas, D., Tsitsiklis, J. 1993. "Simulated Annealing." *Statistical Science*, Vol. 8, No. 1, pp. 10–15.
- Dhillon, S.S., K. Chakrabarty and S. S. Iyengar. 2002. "Sensor placement for grid coverage under imprecise detections." *Proc. International Conference on Information Fusion (FUSION 2002)*, pp. 1581–1587.
- Dhillon S.S. and K. Chakrabarty. 2003. "Sensor placement for effective coverage and surveillance in distributed sensor networks." *Proc. IEEE Wireless Communications and Networking Conference*, pp. 1609–1614.
- Dobossy, M.E., M.A. Celia and J.M. Nordbotten. 2010. "An efficient framework for performing industrial risk assessment of leakage for geological storage of CO₂." *International Conference on Greenhouse Gas Technologies, GHGT-10*, Amsterdam, The Netherlands, September, 2010.

Environmental Protection Agency. 2008. "Geologic CO₂ Sequestration Technology and Cost Analysis." Technical Support Document, EPA 816-B-08-009, June 2008.

Gao, H., and J. Rose. 2006. "Ultrasonic sensor placement optimization in structural health monitoring using evolutionary strategy." *Review of Quantitative Nondestructive Evaluation*, Volume 25, edited by D. Thompson and D. Chimenti, American Institute of Physics.

GoldSim Technology Group. 2006. *GoldSim User's Guide*, Issaquah, WA, 2006.

Guratzsch, R.F., and S. Mahadevan. 2007. "Probabilistic Optimization of Sensor Placement." *Proceedings to IMAC XXV Conference & Exposition on Structural Dynamics*. Orlando, FL, Feb. 19-22, 2007.

Hajek, B. 1988. "Cooling Schedules for Optimal Annealing." *Mathematics of Operations Research*, Vol. 13, No. 2.

Houston, M.H. 2000. "Seismic Fiber Optic Multiplexed Sensors for Exploration and Reservoir Management, Industrial Sensing Systems," Anbo Wang and Eric Udd, Editors, *Proceedings of SPIE 4202*.

Iman R.L. and W.J. Conover. 1980. "Small Sample Sensitivity Analysis Techniques for Computer Models, with an Application to Risk Assessment." *Communications in Statistics: Theory and Methods*, A 9(17): pp. 1749-1842.

Khan, A., D. Ceglarek, and J. Ni. 1998. "Sensor location optimization for fault diagnosis in multi-fixture assembly systems." *Journal of Manufacturing Science and Engineering*, Volume 120, pp.781-792.

Kirkpatrick, S., C.D. Gelatt and M.P. Vecchi. 1983. "Optimization by Simulated Annealing." *Science, New Series*, Vol. 220, No. 4598

Kollat, J., P. Reed, and R. Maxwell. 2011. "Many-objective groundwater monitoring network design using bias-aware ensemble Kalman filtering, evolutionary optimization, and visual analytics." *Water Resources Research* 47, W02529.

Krause, A., J. Leskovec, C. Guestrin, J. VanBriesen, and C. Faloutsos. 2008. "Efficient Sensor Placement Optimization for Securing Large Water Distribution Networks." *Journal of Water Resources Planning and Management*, November/December, 2008.

Meyer, P., A. Valocchi, and J. Eheart. 1994. "Monitoring network design to provide initial detection of groundwater contamination." *Water Resources Research* 30(9): pp. 2647–2659.

Morris, J., R. Detwiler, S. Friedmann, O. Vorobiev, and Y. Hao. 2009. "The large-scale effects of multiple CO₂ injection sites on formation stability." *Energy Procedia* 1:1831–1837.

Murray, R., T. Baranowski, W. Hart, and R. Janke. 2008. "Risk reduction and sensor network design." *Water Distribution Systems Analysis, Kruger National Park, South Africa*, Volume 340, ASCE.

National Energy Technology Laboratory. 2009. "Best Practices for: Monitoring, Verification and Accounting of CO₂ Stored in Deep Geologic Formations." DOE/NETL-311/081508, January, 2009.

National Energy Technology Laboratory. 2011, "National Risk Assessment Partnership: Science-Based Quantification of Risk Profiles. Scientific & Technical Merit." Draft Report DOE/NETL-2011/1469 R0, January 31, 2011.

Nicklow, J. et al. 2010. "State of the art for genetic algorithms and beyond in water resources planning and management." *Journal of Water Resources Planning and Management* 136(4): pp. 412–432.

Nourani, Y. and B. Andresen. 1998. "A Comparison of Simulated Annealing Cooling Strategies." *J. Phys. A: Math. Gen.* 31, pp. 8373–8385.

Oldenburg, C.M., S.L. Bryant, and J.P. Nicot. 2009. "Certification Framework Based on Effective Trapping for Geologic Carbon Sequestration," *International Journal of Greenhouse Gas Control* 3, pp. 444–457.

Ostfeld, A., J.G. Uber and E. Salomons. 2006. "Battle of the Water Sensor Networks: A Design Challenge for Engineers and Algorithms," *Water Distribution Systems Analysis Symposium*, Cincinnati, Ohio, August, 2006.

Saripalli, P., J. Amonette, F. Rutz and N. Gupta. 2006. "Design of Sensor Networks for Long Term Monitoring of Geological Sequestration", *Energy Conversion and Management* 47, pp. 1968–1974.

Schneider, J.J. and M. Puchuta. 2010. "Investigation of Acceptance Simulated Annealing – A Simplified Approach to Adaptive Cooling Schedules." *Physica A*, 389, pp. 5822–5831.

Storck, P., J. W. Eheart and A. J. Valocchi. 1997. "A Method for the Optimal Location of Monitoring Wells for Detection of Groundwater Contamination in Three Dimensional Heterogeneous Aquifers." *Water Resources Research* 33, No. 9, pp. 2081–2088.

Vickers, L., R. Stolkin, and J. Nickerson. 2006. "Computing environmental models aid sensor placement optimization." *Sima / Milcom Conference*, IEEE, Washington D.C.

Vrugt, J. A., and B. A. Robinson. 2007. "Improved evolutionary optimization from genetically adaptive multimethod search." *Proceedings of the National Academy of Sciences* 104(3): pp. 708–711.

Wu, H., M. Siegel, R. Stiefelhagen, and J. Yang. 2002. "Sensor fusion using Dempster-Shafer Theory." *IEEE Instrumentation and Measurement Technology Conference*, Anchorage, Alaska, May 2002.

Wu, H., M. Siegel, and S. Ablay. 2003. "Sensor fusion using Dempster-Shafer theory II: Static weighting and Kalman filter-like Dynamic weighting." *Instrumentation and Measurement Technology Conference*, Vail, Colorado, May, 2003.

Zou, Y. and K. Chakrabarty. 2004. "Uncertainty-Aware and Coverage-Oriented Deployment for Sensor Networks," *J. Parallel Distrib. Comput.* 64 pp. 788–798.

APPENDICES

Note: work cited in the appendices is included in the reference listing of the main report (Section 10).

Appendix 1 Precedents in Sensor Network Optimization Methods

The approach to MVA optimization for geologic carbon sequestration systems described in this white paper draws upon and extends precedents in this domain. It also draws upon an array of approaches that have been applied in other domains, ranging from groundwater and water distribution network monitoring, to surveillance and target location in security and defense contexts, to system failure and fault detection in engineered systems.

Our application extends previous approaches within the geologic carbon sequestration domain by explicitly addressing risk through algorithmically optimizing sensor placement. Saripalli et al. (2006) attempted to identify the spacing and density (or number) of sensors necessary to effectively quantify leakage fluxes and concentrations. However, in contrast to the approach taken in this white paper, their approach was deterministic in that uncertainty was not included in predictions of CO₂ transport and tracer leakage from the geological reservoir being modeled. They acknowledged that receptor zones of greater value would likely warrant closer sensor node spacing, and noted the importance of assessing risk. However, no algorithmic approach to optimization was employed to do so. Morris et al. (2009) focused not on risk *per se*, but rather on physical modeling of multiple injections at a large scale (tens of kilometers) sequestration site. They linked a reservoir flow model to a geomechanical model, enabling them to investigate the potential for fault activation, itself a potential precursor to CO₂ leakage.

In an application to groundwater monitoring, Meyer et al. (1994) developed a design optimization method which, when linked to a groundwater flow and transport model, identified preferred well monitoring networks against three objectives. The objectives were (1) minimizing network cost; (2) maximizing probability of detecting a contaminant leak; and (3) minimizing the extent of contamination when the leak is first detected. The approach considered uncertainty both in the spatial distribution of saturated hydraulic conductivities and location of the leak for a two-dimensional domain. Storck et al. (1997) extended this approach to consider a three-dimensional

model of the domain. In a further extension, Kollat et al. (2011) applied an ensemble Kalman filtering approach that accounted for uncertain and biased model predictions that are conditioned on uncertain data. This last study addresses decisions of whether, in a given time period, samples should be collected from preexisting locations, but the authors note that it could be extended to consider installation of new sampling wells (as is done in the methods reported in this white paper). The approach was demonstrated using a laboratory-based physical aquifer tracer experiment. Six objectives were considered: (1) Minimize monitoring costs; (2) Maximize the information provided to the Kalman filter; (3) Minimize failures to detect the tracer; (4) Maximize the detection of tracer fluxes; (5) Minimize error in quantifying tracer mass; and (6) Minimize error in quantifying the centroid of the tracer plume. Their optimization approach belongs to a class of solution tools termed *multiobjective evolutionary algorithms*, which has been applied in a broad range of water resources-related applications (e.g., Nicklow et al. 2010). For their reported application, this general approach was combined with an emerging new class of evolutionary algorithms termed *probabilistic model building genetic algorithms* in order to address challenges that are unique to optimization problems involving four or more objectives. Vrugt and Robinson (2007) developed an evolutionary optimization approach that performed well for multiple objectives by running multiple algorithms simultaneously while sharing information between them. Their approach has not to our knowledge been applied in a sensor placement application. Formulations considering multiple objectives are under consideration for future applications of the approach presented within this white paper.

The problem of contaminant detection in water distribution systems is characterized by the need to consider, for typical problems, potential sensor placement locations within thousands of junction combinations in the system. Effective solution approaches must be able to cope with option spaces of this problem size. Model performance is also typically evaluated on the basis of multiple criteria. For example, Aral et al. (2009) considered water volume contaminated, time to detection, and detection likelihood, and implemented an approach based on a sorting genetic algorithm. Competing approaches include that by Krause et al. (2008). They used a combination of approaches, including mixed integer programming, simulated annealing, and a greedy algorithm in order to exploit particular features of this type of problem. This problem has also been addressed by federal agencies such as the USEPA, which has developed a publicly available software package called Threat Ensemble Vulnerability Assessment: Sensor Placement (TEVA-SPOT, Berry et al. 2008 See Murray et al. (2008) for an application using TEVA-SPOT.)

In a more general application context, sensor placement is done to achieve effective areal coverage for purposes of surveillance and target location. These concerns are often the focus in security and military applications. In this domain, addressing placement represents a recent advance relative to historical applications that only considered communication between sensors and “sensor fusion” (e.g., Wu et al. 2002, 2003). In sensor communication the primary issue is how sensors share information, while in sensor fusion the primary issue is how to optimally combine information from multiple sensors so that the result is in some sense more informative than if the sensors were used individually. Recent applications attempt to place sensors optimally while considering the following issues: uncertainty associated with whether a sensor will detect a target, preferential coverage of more vulnerable locations, resilience to sensor failures, and the nature of the terrain (e.g., the existence of obstacles).

Dhillon et al. (2002) and Dhillon and Chakrabarty (2003) used a greedy algorithm that optimally added sensors one at a time, in order to optimally improve a miss probability matrix. Using an algorithmic extension to that approach, Zou and Chakrabarty (2004) considered a situation where the precise locations of the sensors are known only within uncertainty limits, as the sensors may have been dropped from an airplane or may have drifted with the current if deployed underwater. Vickers et al. (2006) used a gradient ascent, non-linear optimization technique in a problem in which the environment in the form of a flowing river influences the most effective deployment locations for detecting an object such as a diver moving with the current. Barrett (2007) used genetic algorithms in a similar application. Some of these applications reflect sensors that will have capabilities (e.g., inter-sensor communication) or features (e.g., location uncertainty, movement) not characteristic of the carbon sequestration context. Other issues are either addressed through the placement algorithm (e.g., target detection uncertainty, preferential coverage of more vulnerable locations, existence of geologic obstacles) or operator interpretation of sensor output (including inference resilience in light of sensor failures).

Systems engineering contexts in which the focus is on optimizing sensor placement to maximize probability of detection of failures or faults are another domain of application. Khan et al. (1998) described a case in which both placement and number of sensors was optimized to improve failure detection in automotive body assembly. In their application, a sensor location was desirable if it enabled distinction between a culpable fault and a culpable fixture. Optimization required analysis of six diagnostic vectors that corresponded to potential fault modes lying along six degrees of freedom.

In quite a different kind of problem, Gao and Rose (2006) described a general approach that combined genetic and evolutionary optimization methods to model structural health in potentially many aerospace, civil, and mechanical infrastructure contexts. In an application, they obtained a tradeoff relationship between optimized sensor network performance and the number of sensors for an aircraft wing section in which sensors are placed to detect crack initiation. Guratzsch and Mahadevan (2007) applied structural health modeling to reporting a flight vehicle's condition in real time. Uncertainty was incorporated via random realizations of spatially and temporally uncertain model parameters in a finite element-based modeling analysis that was used to compute the system's response to the various loads. They employed an optimization scheme that was designed for optimization of noisy objective functions that are costly to evaluate due to computational or experimental complexity. This domain typically involves a distinct set of problems compared to the geologic sequestration context. For example, a far greater knowledge of the system and quantity of experimental data is typically available for analysis.

Appendix 2 Supplementary Technical Details

A. Inference Model

The inference model is used to combine evidence obtained from individual sensors. Its role is to determine at what point it would be inferred that a confinement failure has occurred. The inference model is implemented in two ways: first, it has a component that dynamically updates sensor thresholds. Second, it defines various combinations of evidence that must be obtained to infer that confinement failure has occurred. In the absence of these combinations, inference cannot be made.

A.1. Dynamic Updating of Thresholds

A sensor of type A has a pre-defined threshold of B. B is defined in terms of the units of measurement for the stimulus relevant to the sensor type, and it represents the stimulus level that must be achieved for an operator to infer an anomaly. However a anomalous level in a single sensor is insufficient to infer a confinement failure. This requires additional evidence of anomalous activity). B is therefore a statement about our confidence in the evidence provided by the sensor: a reading below B is too noisy for us to infer an anomaly..

We have extended this concept by modeling sensor thresholds as dynamic. Suppose that our initial MVA option consists only of one sensor, of type A. As noted above, we require this sensor to achieve a reading of B for us to believe that anything anomalous is occurring. Now suppose that we place an additional sensor, also of type A, somewhere in the sequestration site remote from the first sensor. Suppose also that both of these sensors register nonzero (i.e., above noise) readings, but both readings are below B. It is plausible to suggest that, even though B is not exceeded, we have stronger evidence of anomalous activity than in the case of an individual sensor reading below B. That is, we now have two nonzero readings in distinct locations. This suggests that we lower the threshold B: the sensors, by virtue of their nonzero readings and distinct locations, reinforce the inference of a confinement failure. As a result, a stimulus level below B can be sufficient to reinforce inference of a confinement failure.

This example can be extended by considering the addition of a sensor of type A'. Similar reasoning suggests that if this new sensor also registers a nonzero reading we

do not need to require evidence as strong as B from the first sensor. The inference model works in this way by reducing sensor thresholds if certain other sensors register nonzero readings. Note that this is a preliminary inference model and we anticipate significant modifications to reflect more realistic decision-making criteria.

A.2. Combinations Required for Leak Inference

In addition to dynamically updating sensor thresholds, the inference model also checks for specific combinations of exceeded thresholds. The idea is that a reading in excess of a sensor's threshold (initial or updated threshold) is not sufficient to infer that confinement failure is occurring – it is only sufficient to infer an anomaly. Multiple anomalies must be detected to confidently infer that leak has occurred, as mitigation is a potentially costly process and should not be attempted without strong evidence for its necessity.

B. Optimization Model

As discussed, our tentative consequence metric is time to detection, and this is evaluated for a given MVA design option with respect to several confinement failure scenarios, each representing a single Monte Carlo sample member from the underlying risk model. The constraints currently modeled are cost constraints, and we recognize the possibility of imposing additional constraints in future, such as geographical constraints upon the locations of the sensors.

The mathematical formulation of the problem is as follows:

$$\begin{aligned} \text{Min}_{\mathbf{x}} \text{TTD}(\mathbf{x}) \quad \text{s.t.} \\ C(\mathbf{x}) \leq \alpha \end{aligned} \tag{2.1}$$

Where TTD is the function used for evaluating time to detection, C is the cost function, α is the cost constraint, and \mathbf{x} is the variable representing alternative MVA design options.

The TTD function itself can be represented as follows:

$$\text{TTD}(\mathbf{x}) = \sum_i p_i T_i(\mathbf{x}) \tag{2.2}$$

where $T_i(\mathbf{x})$ represents the time it takes MVA option \mathbf{x} to detect leak corresponding to scenario i , and p_i represents the probability of scenario i (in the numerical implementation, each scenario is represented by an equiprobable Monte Carlo sample member). Note that $T_i(\mathbf{x})$ is the time to detection measured from the onset of that confinement failure – it is *not* the time to detection measured from the beginning of the injection period. For instance, if leak scenario i does not involve actual leakage until time period N , and MVA option \mathbf{x} detects that leak at time $N+M$, the value of $T_i(\mathbf{x})$ will be M .

The reason simulated annealing was chosen as the optimization technique is related to the nature of the objective function. While the TTD function is itself a linear combination of individual $T_i(\mathbf{x})$ functions, these individual functions themselves cannot necessarily be expressed as linear functions, or indeed as any functions with closed form expressions. Each of these functions is evaluated by querying a database of scenario data against sensor types and locations found in \mathbf{x} . It is possible that this is highly nonlinear: if there is a geologic impediment to CO_2 flow, for example, an MVA option placed on one side of the impediment will yield a finite time to detection, but a slight shift of that option to the other side of the impediment will not yield no detection at all. In addition, future versions of the objective function may involve different consequence metrics which can also be nonlinear. Simulated annealing is a good technique for optimization problems with so-called “black box” objective functions, such as this one. The technique does not require differentiation or any other mathematical operation to be applied to the objective function. It only requires us to be able to evaluate the objective function for the feasible candidate solutions.

B.1 Cost–Objective Analysis of MVA Design Options

While the objective function as described above is an expected time to detection (mean over the Monte Carlo sample), we allow for the possibility of incorporating cost directly into the objective function. More specifically, the user has the option of entering a nonzero number in the Cost Coefficient section of the user input page. If this is done, then the objective function becomes

$$\text{TTD}'(\mathbf{x}) = \text{TTD}(\mathbf{x}) + \beta C(\mathbf{x}) \quad (2.3)$$

where β is the number entered by the user (representing a cost/risk tradeoff). In this case, the rest of the inputs and algorithm operation are the same as they were before –

the only difference is in the way in which different MVA design options are compared. The rationale behind this approach is to discount design options that provide little reduction in time to detection at high cost.